UC Santa Barbara

Title
Interaction Forces between Supported Lipid Bilayers in the Presence of PEGylated Polymers

Authors
Banquy, Xavier
Lee, Dong Woog
Kristiansen, Kai
et al.

Interaction Forces between Supported Lipid Bilayers in the Presence of PEGylated Polymers

Xavier Banquy,*[,†] Dong Woog Lee,[‡] Kai Kristiansen,[‡] Matthew A. Gebbie,[§] and Jacob N. Israelachvili*[,‡,§]

[†]Canada Research Chair in Bio-Inspired Materials, Faculté de Pharmacie, Université de Montréal, C.P. 6128, Succursale Centre-ville, Montréal, Québec H3T1J4, Canada

[‡]Department of Chemical Engineering and [§]Materials Department, University of California Santa Barbara (UCSB), Santa Barbara, California 93106, United States States

S *Supporting Information*

ABSTRACT: Using the surface forces apparatus (SFA), interaction forces between supported lipid bilayers were measured in the presence of polyethylene glycol and two other commercially available pegylated triblock polymers, Pluronic F68 and F127. Pluronic F68 has a smaller central hydrophobic block compared to F127 and therefore is more hydrophilic. The study aimed to unravel the effects of polymer architecture and composition on the interactions between the bilayers. Our keys findings show that below the critical aggregation concentration (CAC) of the polymers, a soft, weakly anchored, polymer layer is formed on the surface of the bilayers. The anchoring strength of this physisorbed layer was found to increase significantly with the size of the hydrophobic block of the polymer, and was strongest for the more hydrophobic polymer, F127. Above the CAC, a dense polymer layer, exhibiting gel-like properties, was found to rapidly grow on the bilayers even after mechanical disruption. The cohesive interaction maintaining the gel layer structure was found to be stronger for F127, and was also found to promote the formation of highly structured aggregates on the bilayers.
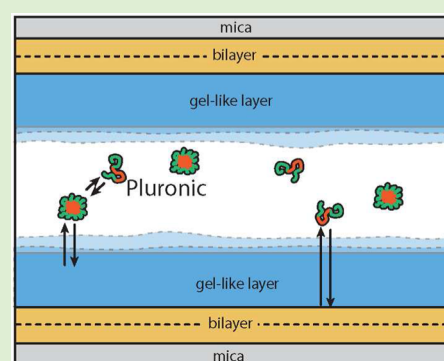
INTRODUCTION

Multiblock polymers composed of poly(ethylene oxide) (PEO) have gained increasing attention in a wide range of biomedical applications. One example of that is their extensive use in the development of drug delivery systems that are able to evade recognition by the arsenal of proteins involved in the immune response to foreign bodies.[1−3] More recently, it has been suggested that linear multiblock polymers based on polyethylene and polypropylene glycol (PEO and PPO) could be used to tune the stability of liposomal formulations[3] or to repair damage to cellular membranes.[4,5] Interestingly, the strong affinity of such polymers to cell membranes has also been shown to regulate certain proteins activity such as P-glycoprotein efflux pump.[6,7]

The most commonly used PEO/PPO-based multiblock polymers belong to the Pluronic family, also known as Poloxamer. This commercially available family of polymers, some of which are approved for medical use by the FDA, has been tested in many biomedical studies. The most commonly tested Pluronics include Pluronic F68, which has been shown to be a very potent suppressor of carcinogenesis in the colon of rats and mice,[8] Pluronic F127, which demonstrated the ability to penetrate cellular membranes and to stabilize them after being subjected to an external stress,[9] and Pluronic P85, which has been shown to significantly enhance drug permeability through epithelial cells.[10]

Due to the many beneficial biological and biomedical properties of Pluronics that have been reported to date, we decided to characterize the interactions forces between Pluronics and lipid membranes using a surface forces apparatus (SFA) to provide a molecular level understanding of the interaction forces that may be at the origin of these reported properties.

The SFA enables one to measure and quantify interaction forces between supported lipid bilayers in aqueous media,[11] and previous studies have shown that electrostatic, van der Waals and hydrophobic interactions between bilayers could be characterized precisely using this technique.[12] In the present study, we report the characterization of the interaction forces between myelin lipid bilayers in the presence of different polymers including PEG, Pluronic F68, and F127. The selection of myelin lipid bilayers was motivated by recent reports showing that such polymers could re-establish neuronal signal transmission after severe mechanical damage of the spinal cord in rats.[13−15] These results suggest that the same polymers could be used in other severe pathologies of the central nervous system (CNS) particularly affecting the myelin sheath such as multiple sclerosis (MS). In MS, the myelin membrane wrapping the axon loses structural integrity by swelling and vesiculation, a process called demyelination. The use of Pluronic polymers could be beneficial in re-establishing the molecular forces between the myelin membranes necessary to stabilize the structure of the myelin

Table 1

Name	Structure	Average molecular weight*	Hydrodynamic diameter**	Unperturbed radius of gyration of single chain	Critical Aggregation Concentration
		M_w (g/mol)	D_H (nm)	R_g (nm)	(CAC)
PEG	Homopolymer n=180	8000 (7000 to 9000)	3-4	4.1 (Ref. 17)	--
Pluronic F68	Triblock polymer PEO-PPO-PEO n=80 n=27 n=80	8400 (7680 to 9510)	4[18]	1.9 (Ref. 19)	0.48 mM 0.4 w/w% (Ref. 20)
Pluronic F127	Triblock polymer PEO-PPO-PEO n=101 n=56 n=101	12600 (9840 to 14600)	5-7	2.2 (Ref. 18)	0.0028 mM 0.0035 w/w% (Ref. 20)

*Provided by the manufacturer. **Measured by DLS at $C > CAC$.

and its biological function. This study therefore aims to establish the fundamental molecular mechanism governing the interaction (adhesive or repulsive) of lipid membranes in the presence of different PEGylated polymers.

■ MATERIALS AND METHOD

Materials. The lipid composition of the biomembranes used in this study was chosen based on previous work,[16] where differences in lipid compositions of the white matter of healthy marmosets compared to marmosets suffering experimental allergenic encephalomyelitis (EAE) were identified. The lipid composition of the membrane was 7.4 mol % of phosphatidylserine (porcine brain PS−), 2.2 mol % of sphingomyelin (porcine brain SM), 20 mol % of phosphatidylcholine (porcine brain, PC), 3.3 mol % of phosphatidylethanolamine (porcine brain PE), and 37 mol % of cholesterol (ovine wool, Avanti Polar Lipids, Alabaster, AL, purity >99%). The fatty acid chain lengths of the three major lipids (PC, PE and PS−) are 16:0, 18:0, 18:1 and 20:4. All lipids were stored in chloroform until use. Lipids were used as received without any further characterization. Dipalmitoylphosphatidylethanolamine (DPPE), sodium nitrate (purity ≥99.0%), morpholine-propanesulfonic acid (Mops) sodium salt (purity ≥99.5%), and calcium nitrate (purity ≥99.0%) were purchased from Sigma-Aldrich (St. Louis, MO). The following solvents were used to disperse lipids: hexane (RegentPlus, purity ≥99.0%), chloroform (CHROMASOLVE Plus, for HPLC, purity ≥99.9%), ethanol (200 proof, HPLC/spectrophotometric grade), and methanol (CHROMASOLVE Plus, for HPLC, purity ≥99.9%) (Sigma-Aldrich, St. Louis, MO).

Polymers were purchased from Sigma-Aldrich (St. Louis, MO) and were used as received. The physical chemical properties of the polymers are given in Table 1.

Measurements of the Interaction Forces Using the SFA. The Surface Forces Apparatus model 2000 (SFA 2000, SurForce LLC)[21] was used in this study for accurate force–distance measurements and line image of the bilayer–bilayer contact area. Figure 1 shows a schematic of the experimental configuration used for measuring the interaction forces between the supported bilayers in the SFA. The two lipid bilayers were prepared using the Langmuir–Blodgett (LB) deposition technique as described previously[22−24] and transferred into the SFA chamber (which was previously filled with liquid) in small beakers in order to keep the bilayers constantly immersed in aqueous solution.[11,25] The upper surface was installed on a fixed solid mount, while the lower surface was mounted in a small cup (3 mL) supported by a double cantilever (force-
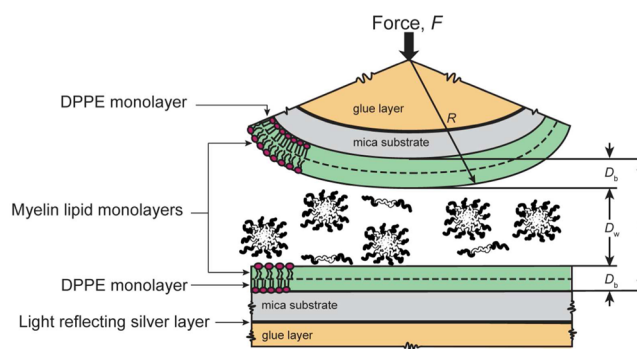
Figure 1. Schematic representation of the experimental configuration used in this study. Each lipid bilayer was made of one DPPE leaflet in contact with the mica surface and one myelin lipid leaflet exposed to the medium. Different polymer solutions were tested as the medium in order to assess the impact of chain adsorption/depletion on the intermolecular forces between bilayers.

measuring) spring. This configuration enabled the replacement of the entire solution in the SFA chamber (180 mL) with a new solution of polymer without exposing the bilayers to air. This procedure was used to increase the concentration of polymer, C, in the surrounding media without changing contact position or surfaces. An equilibration time of 1 h was given to the surfaces after each change of solution (or increment of concentration) before starting the measurements.

The separation distance between the two surfaces was measured as previously described using multiple beam interferometry.[26] Briefly, a white light beam is directed normal to the surfaces, and the interference fringes generated from the reflections of the light beam between the two back-silvered mica sheets are analyzed in a spectrometer equipped with a digital camera (Hamamatsu Orca 03G, USA). The separation distance D between the surfaces is calculated (to ±1 Å) from the wavelength λ of the interference fringes (also called fringes of equal chromatic order, FECO) using the equation:[26]

$$\tan(k\mu_w D) = \frac{2\bar{\mu} \sin(n\pi\Delta\lambda_n/\lambda)}{(1 + \bar{\mu}^2) \cos(n\pi\Delta\lambda_n/\lambda) \pm (\bar{\mu}^2 - 1)} \tag{1}$$

where μ_w is, as a first approximation, the refractive index of water, and $\bar{\mu}$ is the ratio of the refractive indices between mica and the solution

between the mica surfaces (water) at λ. The distance resolution in our experiments was about 0.1−0.2 nm, which depended mostly on the mica sheets thickness and alignment of the optical setup.

The normal interaction force F between bilayers as a function of the mica−mica separation distance D was obtained by measuring the deflection of the double cantilever spring with a known spring constant supporting the lower surface.[11,12,27] In particular, the local geometry of the contact zone as well as the shape of the interacting surfaces was extracted from the analysis of the FECO fringes with a normal resolution of 0.1−0.2 nm and a lateral resolution of 1 μm.[28,29]

Most of the experiments were repeated at least twice. Due to the strong time dependency of the measured interactions, the force runs presented in this report should not be seen as a *quantitatively* accurate measure of the state of the system, but rather as a snapshot of the state of an evolving system. On the other hand, the values of the decay length and hard wall thickness were found to be reproducible to better than 1.5 nm.

DLS Measurement. The hydrodynamic diameter D_H of the polymers was measured using dynamic light scattering on a Zetasizer from Malvern. The polymer solution was prepared at a concentration 10 times higher than the critical aggregation concentration in Mops buffer, filtrated through 0.2 um filter membrane and inserted in the measurement cuvette. Measurements were performed at a scattering angle of 173°, at room temperature. Results reported in Table 1 correspond to the z-average value of three independent measurements of 10 runs each.

RESULTS AND DISCUSSION

Interaction Forces in the Presence of PEG. The interaction forces between freshly deposited lipid bilayers were first measured in pure buffer (Figure 2A, Figure S1). The interaction force profile, which represents the variation of the interaction force normalized by the curvature of the surfaces as a function of the separation distance between the two mica surfaces, was observed to be purely repulsive. The origin of this repulsive interaction was found to be electrostatic and was quantitatively described using the linearized DLVO theory applied to two bilayers in an electrolyte solution.[23] The experimental Debye length, the characteristic screening length of the electrostatic force due to bulk electrolyte, was found to be 8.0 Å (see Figure S1), which is in excellent agreement with the theoretical value of 7.8 Å obtained using the Graham equation for a dilute electrolyte solution at a concentration of 150 mM.[12]

Once the bilayers were immersed in a solution of PEG at 10 % w/w, many features of the force profile change. After 4 h of immersion (see Figure 2A), the measured forces were no longer purely repulsive, but presented a small attractive minimum that could be detected on approach and on separation of the surfaces. On the approach, the surfaces jumped into soft contact over a separation distance ΔD_j, which depended weakly on the immersion time, t. After 4 h of immersion, ΔD_j was found to be close to 4.2 ± 0.2 nm and stayed almost constant to 4.6 ± 0.2 nm after 6 h of immersion. These values are in close agreement with the value of R_g obtained for this polymer (see Table 1) suggesting that the attractive interaction force at the origin of the jump to contact of the surfaces is as expected for a depletion force.

Rigorously, the ΔD_j should be compared to the correlation length of the polymer in order to confirm that the measured interaction is indeed a depletion interaction. In dilute solution, the correlation length is close to the R_g of the polymer, while in the semidilute regime, which is presently the case, the correlation scale is smaller. The contraction factor is expected to scale as $(C/C^*)^{-1/8}$, C^* being the overlap concentration, which in our case gives a value of 0.91. Therefore, the expected correlation length
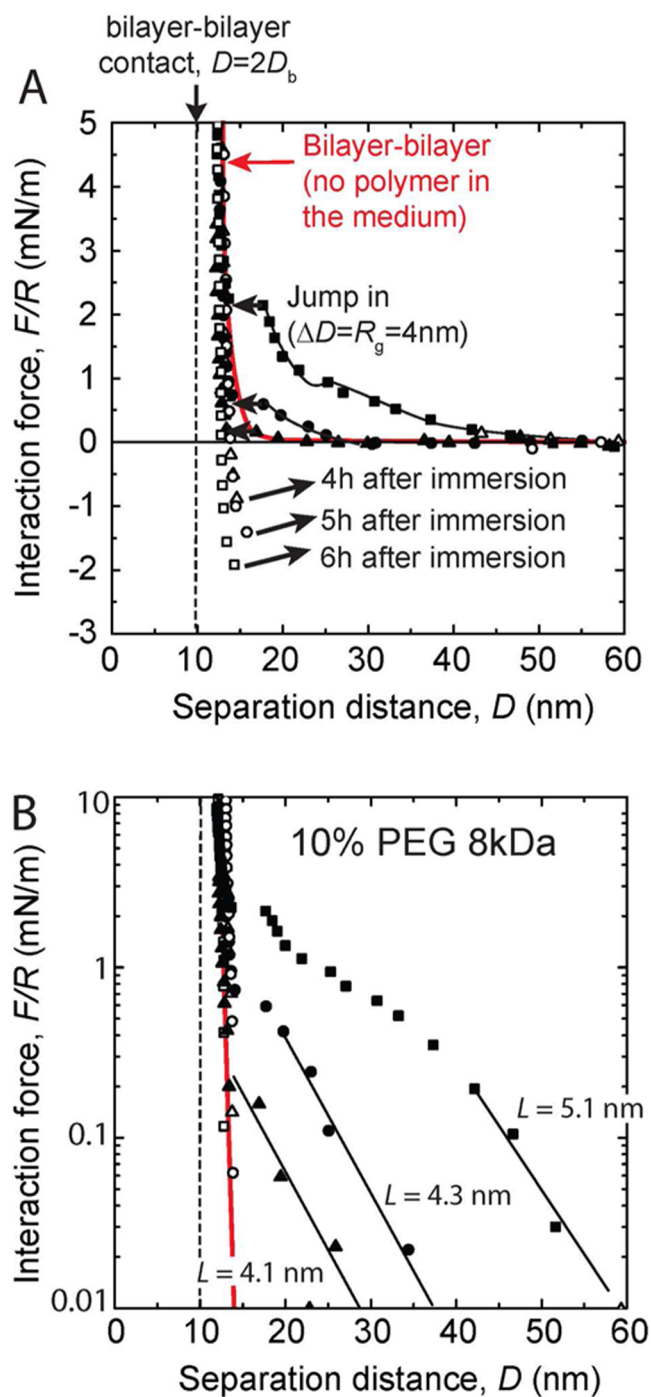
Figure 2. Interaction forces between two myelin lipid bilayers in the presence of a PEG 8 kDa solution at 10 %w/w in buffer presented on a linear scale (A) and log scale (B). The interaction forces were systematically repulsive on the approach of the surface until a sudden jump into contact occurred at a separation distance between the bilayers close to R_g. As the immersion/adsorption time increases, the repulsion on the approach and the adhesion on separation become stronger, indicating a slow structuring process of the polymer solution at the bilayer−water interface.

of our system is expected to be 3.8 nm, which is still in good agreement with the measured value of ΔD_j.

As the immersion time t increased from 4 to 6 h, the interaction forces become increasingly repulsive on the approach of the surfaces and exhibit smooth oscillations, suggesting that

the polymer molecules were gradually forming layers at the bilayer—water interface. Such behavior is not surprising considering that oscillatory forces systematically arise once there is a change in density at the surface and therefore do not require any attractive polymer—polymer or polymer—surface interaction.

The reason why layering occurs only between 4 and 6 h of immersion is still unclear. It certainly suggests that immersion time is not the only factor controlling the layering process and that other factors, such as the number of compression/decompression cycles and the approach/separation speed,[30] might also be involved.

The observed time dependence is peculiar for a depletion interaction but not impossible considering that it involves a concentrated polymer solution and a thin film equilibrating with a reservoir solution by diffusion only. Interaction phenomena between surfaces or lipid bilayers in the presence of semidilute to concentrated polymer solutions have been reported repeatedly to strongly depend on the immersion/incubation time.[31] Due to the very slow dynamics associated with such systems, the measurement of the interaction forces with the SFA can be seen as a snapshot of the interaction as it evolves toward thermodynamic equilibrium. Our experiments suggest that such equilibrium can be reached after at least 5 h of immersion of the surfaces.

The adhesive force measured at the jump out instability increased from $F_{ad}/R = -[F/R]_{min} = 0.9$ mN/m at $t = 4$ h to $F_{ad}/R = 2$ mN/m at $t = 6$ h which, in terms of adhesion energy, E_{ad}, corresponds to a increase of $E_{ad} = F_{ad}/2\pi R = 0.1$ mJ/m^2 to $E_{ad} = 0.3$ mJ/m^2, respectively. From these values, an effective osmotic pressure, Π (calculated considering that the interaction energy is only due to the depletion interaction) can be estimated by $\Pi = E_{ad}/(D_{jump-out} - D_{jump-in})$, where $D_{jump-in}$ and $D_{jump-out}$ are the separation distances at jump in and out of contact, respectively. The effective osmotic pressures measured by SFA (see Table 2) at $t = 5$ h and 6 h were close to the value of $\Pi = 1.2-1.3$ atm obtained by ultracentrifugation.[32]

Table 2. Interaction Energies and Respective Effective Osmotic Pressure Values Obtained from the Force Profiles Shown in Figure 2

immersion time, t (h)	adhesive energy, E_{ad} (mJ/m^2)	osmotic pressure, Π (atm)
4	0.1	0.6 ± 0.2
5	0.2	1.1 ± 0.2
6	0.3	0.9 ± 0.2

These results confirm that the attractive force measured between the lipid bilayers is indeed a depletion force. These observations are very similar to previous SFA results reported on dimyristoylphosphatidylcholine (DMPC) membranes by Kuhl et al. using the SFA.[32,33] In addition to the attractive depletion force, the authors also reported long-range and time-dependent repulsion forces of electrostatic origin, at least for polymers with molecular weights higher than 18 000 g/mol. At such high molecular weights, the authors proposed that the PEG chains are able to complex free ions in solution in a similar manner to crown ethers, which in turn significantly affects their conformation at the bilayer—water interface. Such a phenomenon is expected to be much less pronounced with PEG chains of lower molecular weight as in our situation.

Our experiments showed that the repulsive forces can be fairly well described by a single exponential force law with a decay length of R_g (see Figure 2B), which is expected for the interaction force between two layers of grafted PEG chains in the "mushroom" conformation.

The fact that the decay length of the interaction is slightly larger than the expected correlation length of the polymer solution (which is close to R_g) suggests that other phenomena might be involved in this long-range interaction. We can speculate that the slow squeeze out of the polymer from the confined space, as well as fluctuations in the polymer conformation might contribute to such differences.

Our observations suggests that the observed repulsive interaction force is due to the slow layering of the PEG solution in the vicinity of the bilayer—water interface. This was also suggested by the smooth oscillations in the long-range repulsive portion of the force profile observed after 6 h of immersion.

We noticed that in the region of the force profile where the polymer is squeezed out of the contact, the repulsive portion of the profile ($D < 15$ nm) is purely exponential with an associated decay length of 7.5 Å, which is close to the expected Debye length of 7.8 Å. This confirms that in the depleted region, the main contribution to the interaction force between the bilayers is the overlapping of the electrostatic double layers of each interface. To avoid irreversible damage of the bilayers, these were not highly compressed, which prevented us from unambiguously quantifying other contributions to the interaction forces such as steric-hydration forces.

Interaction Forces in the Presence of Pluronic F68. The interaction forces between the lipid bilayers in the presence of Pluronic F68 exhibit many differences compared to the forces measured in the presence of PEG. When the bilayers were exposed to a solution of F68 at 0.01 %w/w (Figure 3A), which is well below the critical aggregation concentration (CAC) of the polymer (see Table 1), purely repulsive interaction forces were observed both on approach and separation of the surfaces. The onset of the repulsion was found to start at $D \approx 25$ nm, and shifted in to smaller surface—surface separation distances after repeated approach/separation cycles. Interestingly, the interaction forces were found to follow a single exponential decay law, at least for the second and third approach/separation cycles (Figure 3A). The decay length, L, was found to be very close to the theoretical value of the Debye length λ_D of the medium ($\lambda_D = 0.8$ nm), suggesting that no surface-bound polymer aggregates are present on the bilayers during the second and third approach/separation cycles. Such behavior can be explained by the F68 forming weakly bound polymer aggregates that are mechanically removed/displaced during the first approach of the surfaces and do not readsorb on the bilayers during the time frame of the experiment. Notably, this observation does not rule out the possibility that some fraction of the F68 polymers have inserted into the bilayers.

The measured thickness of a bilayer under high compression ($F/R = 16$ mN/m, $P = 2.5$ MPa) was found to be 0.5 nm thinner than in the absence of the polymer. Such thinning of the bilayers can be explained by a slight fluidization of the bilayers either due to the insertion of the polymer into the membranes as suggested by recent MD studies[34] or to the solubilization of the lipids by the polymer.[35] Fluidization of the bilayers can also lead to changes in the hydration of the lipid head groups, which could be another contribution to the change in bilayer thickness.

When increasing the concentration of polymer in the solution, C, by 10-fold (Figure 3B), both the thickness of the bilayer and
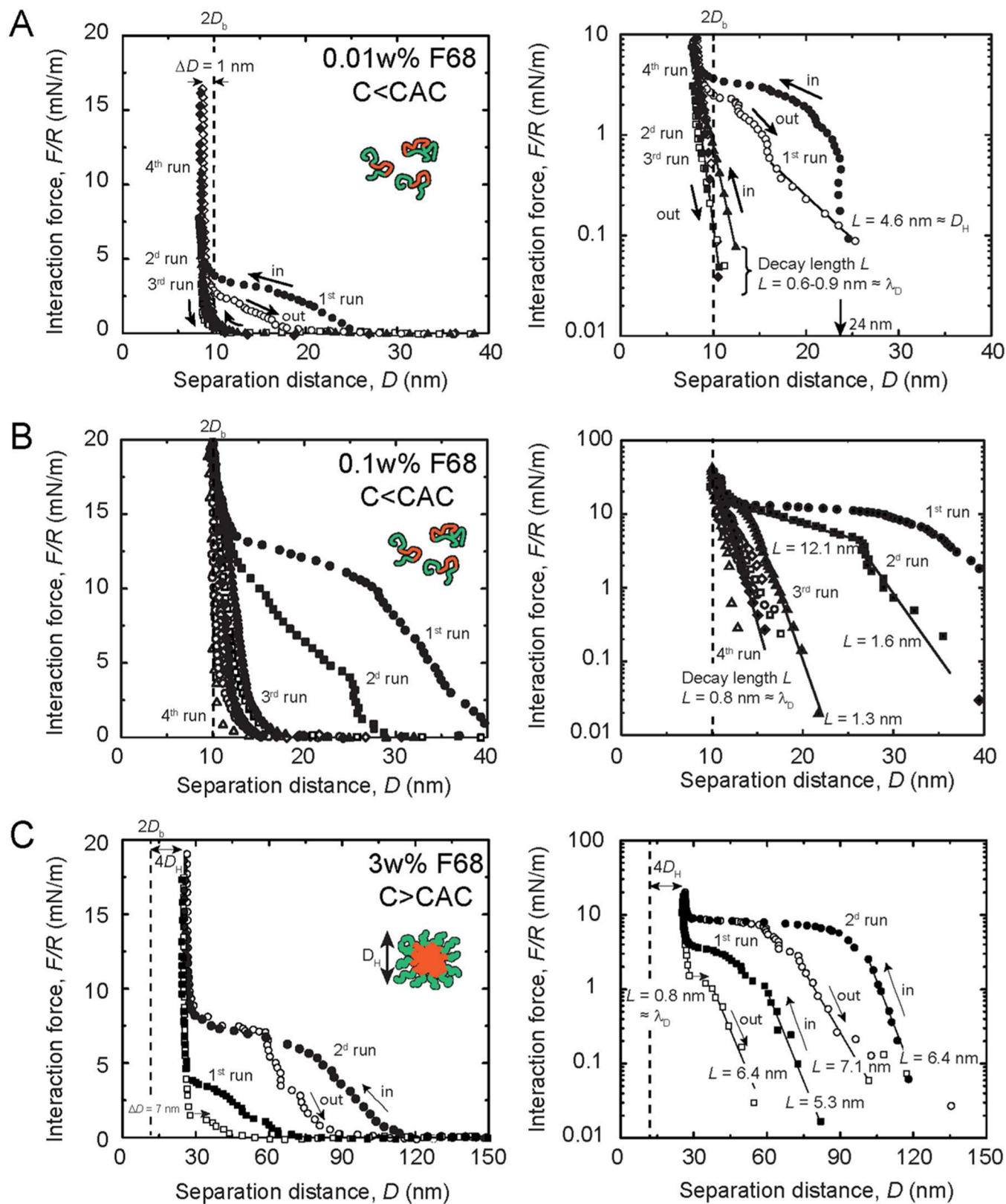
Figure 3. Interaction forces between supported lipid bilayers in the presence of Pluronic F68 at increasing concentration, C (from A to C). Interaction forces are presented on a linear scale (left panel) and a log scale (right panel).

the onset of the interaction forces were found to significantly increase. The onset of the interaction forces was still strongly dependent on the history of the contact, showing long-range repulsion starting at more than 40 nm on the first approach, and

decreasing to 15 nm on the fourth approach. The measured thickness of the bilayers was found to be independent of the cycle number and slightly thicker than at a polymer concentration of 0.01%, suggesting that the polymer chains are strongly adsorbed
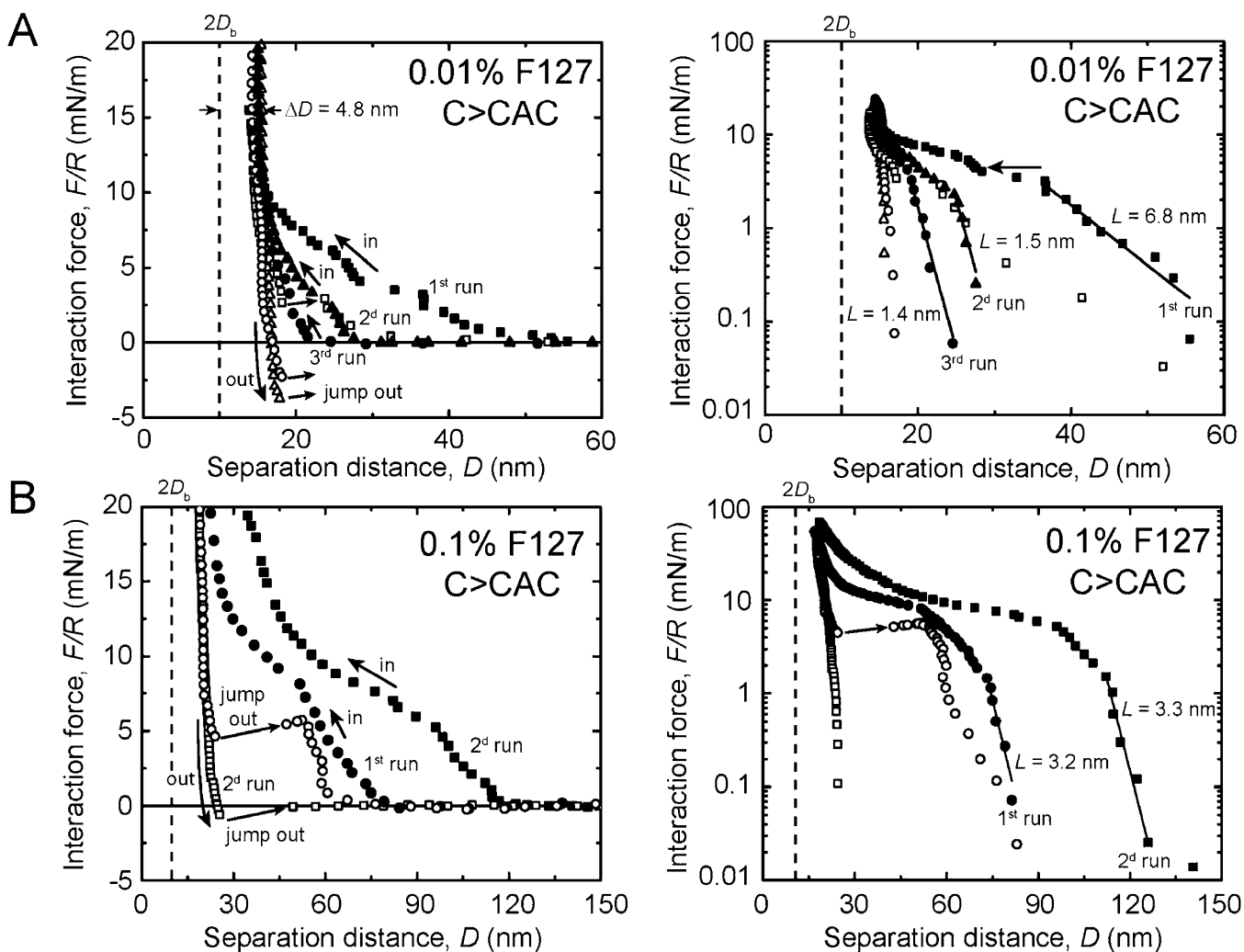
Figure 4. Interaction forces between supported lipid bilayers in the presence of Pluronic F127 at increasing concentration, C (A,B). Interaction forces are presented on a linear scale (left panel) and a log scale (right panel).

to the bilayers. These observations can be explained considering that the affinity of the polymer to the bilayers is essentially mediated by the hydrophobic interaction between the central hydrophobic block of the polymer and the hydrocarbon inner core of the bilayer, which after fluidization of the bilayers, is more exposed to the external medium (Figure 3).[34,36,37]

The interaction force profiles shown in Figure 3 exhibit interesting features, especially during the first three approach/separation cycles. During these cycles, the interaction forces presented a plateau in the force at separation distances ranging from 30 to 25 to 10 nm for the first two cycles and 15 to 10 nm for the third. The plateau was much more pronounced during the first cycle than on subsequent cycles, which is a clear indication that compression of the bound polymer layers induces a dramatic structural change of the adsorbed polymer layers. This polymer layer is expected to be formed by polymer chains and submicellar aggregates interacting via weak intermolecular bonds such as hydrogen bonds and segment−segment hydrophobic interactions, potentially leading to a percolated network. The long-range portion of the interaction force profiles appeared to follow a single exponential decay force law of characteristic decay length $L = 1.3−1.6$ nm, which is very close to the theoretical value of the radius of gyration, $R_g = 1.3$ nm, of a single PEO block of Pluronic F68. These observations suggest that the interface between the

adsorbed polymer layer and the polymer solution is mostly composed of PEO chains in the weakly adsorbed random coil conformation.

It is interesting to note that the polymer layer formed on the bilayers was found to be weakly bound to the bilayers. During the fourth approach/separation cycle, the interaction forces showed a characteristic decay length equal to the Debye length, suggesting that the polymer layer present on the bilayers did not have time to reform in the time frame of the measurement cycle.

At a C of 3 %w/w, which is well above the CAC of the polymer (see Table 1), the purely repulsive interaction force profiles were dramatically shifted to larger separation distances (Figure 3C). During the first approach/separation cycle, the onset of the interaction force was around 80−90 nm, and the hard wall thickness was located at 26 nm, which corresponds to an interbilayer film thickness of approximately $4D_H$. At the second approach/separation cycle, the onset of the interaction force was shifted to an even larger separation of 130 nm, a striking difference from the situations observed at polymer concentrations below the CAC. The force profiles still present a pronounced plateau at forces varying from 5 to 10 mN/m depending on the run cycle, and a decay length on approach and separation varying between 5 and 7 nm. Interestingly, the shape

of the FECO fringes acquired at soft or hard contact ($F/R > 20$ mN/m) did not exhibit any particular local deformation that could be due to the presence of polymeric aggregates (this point is discussed in detail later). After the second cycle, the onset of the interaction forces was still shifted to much larger separation distances estimated to be a few microns (not represented in Figure 3C).

These observations suggest that at polymer concentrations higher than the CAC, a polymer layer builds up rapidly and remains strongly bound to the bilayers. The nature of this polymer layer could be similar to the one observed at lower polymer concentrations but composed of larger micelles or cylindrical micelles (see Figure 4).

Interaction Forces in the Presence of Pluronic F127. As shown in Table 1, Pluronic F127 exhibits a significantly longer hydrophobic central block compared to F68, but with similar hydrophilic end-blocks. As a consequence, the CAC of the polymer is 2 orders of magnitude smaller than F68, and the hydrodynamic diameter of the aggregates in solution is about 5−7 nm, slightly larger than F68. The interaction forces between bilayers in the presence of F127 at a concentration C slightly larger than the CAC presents certain features that are similar to those measured in the presence of F68: at $C = 0.01\% \gtrsim$ CAC, the onset of the interaction decreases with the number of approach/separation cycles from 80 to 27 nm. The long-range interaction forces are well described by a single exponential decay with a decay length L decreasing from 6.8 to 1.4 nm from the first to the third approach/separation cycle, well above the Debye length of the medium. Interestingly, on the approach, the force profiles present few "jump in" instabilities that indicate the sudden squeeze out of polymer layers/aggregates from the contact region. Contrarily to F68, we also noticed that the position of the hard wall obtained with F127 at $C = 0.01$ %w/w is significantly larger, which supports the above conclusion that a strongly anchored polymer layer was present at the surface of the bilayers.

On separation, adhesive forces were systematically measured and found to increase with the number of separation cycles and immersion time. During the first separation, a small jump out instability was observed at $F/R = 2.5$ mN/m, corresponding to a local minimum in the interaction force profile (see Figure 4A). The associated adhesive force was very small and estimated to be <0.1 mN/m.

Interestingly, our results show that the adhesion force associated with such a local minimum increases with the incubation time. After 4 h of incubation (second run), the measured adhesion force was $F_{ad}/R = -2.5$ mN/m ($E_{ad} = 0.4$ mJ/m^2), increasing to $F_{ad}/R = -4$ mN/m ($E_{ad} = 0.6$ mJ/m^2) after 6 h of incubation (third run). The position of the hard wall did not change during these measurements as expected, in a first approximation, for depletion forces. These observations lead us to conclude that the observed depletion interaction is due to a slow structuring of the bound polymer layer at the two interfaces.

As shown in Figure 4B, increasing the F127 polymer concentration to 0.1 %w/w altered the interaction force profiles in a similar way to F68. The onsets of interaction were found to increase with the approach/separation cycle or incubation time, and the decay length L of the long-range portion of the interaction force was found to remain fairly constant, around 3 nm.

The force profiles were characterized by a large plateau occurring at a force of $F_{ad}/R \sim 7.5-10$ mN/m ($E_{ad} = 1.2-1.6$ mJ/m^2) that extends between 30 and 50 nm for the first run and increased to 45−90 nm for the second run. A third run was

measured that shows an onset of the interaction larger than a micron (not shown in Figure 4B). Adhesion forces were also measured and are found to follow a similar trend compared to the 0.01 %w/w solution (see Figure 4B). A small local minimum (located in the repulsive/positive force region of the force run) was first measured during the first run giving a net adhesion force of $F/R = -1$ mN/m which increases slightly to -1.2 mN/m on the 2^d run, but now appears in the attractive (negative) force region.

Analysis of the shape of the FECO fringes during "hard" compression of the bilayers in the presence of Pluronic polymers at $C \gg$ CAC reveals subtle differences in the behavior of the two polymers tested. Figure 5A shows FECO fringes obtained from a
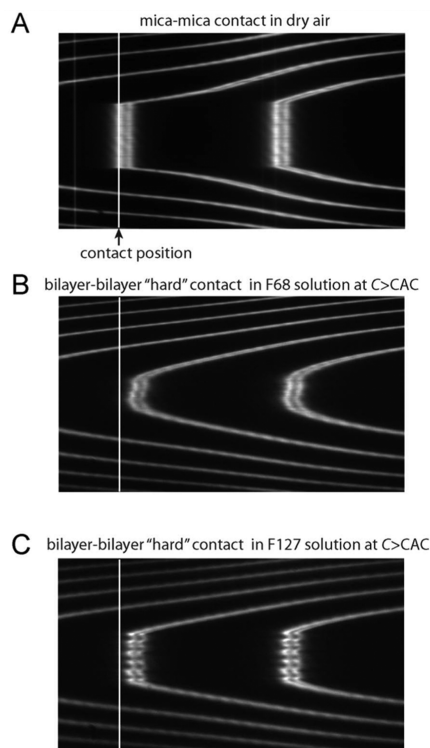
Figure 5. FECO images obtained at (A) mica−mica contact in dry air, (B) bilayer−bilayer contact in the presence of F68, and (C) bilayer−bilayer contact in the presence of F127. These pictures were taken during two separate experiments using mica substrates of identical thickness. The applied force to obtain the flat contact region was $\gtrsim 100$ mN/m.

flat contact between two bare mica surfaces in dry air, prior to the bilayer deposition. In the presence of the bilayers and in F68 solution (Figure 5B), the shape of the fringe in "hard" contact ($F/R > 100$ mN/m) exhibits a smooth, weakly deformed, contact area characteristic of a homogeneous interfacial film. In the presence of F127, the contact area exhibits pronounced deformations with quasi periodic ripples, suggesting the presence of a heterogeneous polymer layer composed of stiff aggregates able to deform the mica surfaces even under high compression. These observations suggest that F68 and F127 assemble into very different structures at the bilayer surface.

■ DISCUSSION

Our experimental observations can be summarized as follows:

- PEG with a molecular weight of 8 kDa does not adsorb on the lipid bilayers, in agreement with the work of Kuhl et

al.[33] Between two lipid bilayers, immersed in PEG 8 kDa solution, an attractive energy minimum is attributed to the depletion force. Evidence of gradual polymer layering/structuring after long immersion times appears to coincide with the increase of the depletion attraction.

- Below or close to the CAC, the adsorbed Pluronics exhibit repulsive forces on the approach (see Figure 4) with an onset distance that decreases with the experimental runs and/or immersion time. On the first approach/separation cycle, a weakly bound polymer layer is systematically found on the bilayers, which are in turn slightly thinner/fluidized by the presence of the adsorbed polymer. The decay length of the long-range decay of the force profiles scales fairly well with the radius of gyration, R_g, of the isolated chains, at least for the first few experimental runs (when the polymer is still present on the surface). All the interaction forces measured on separation were purely repulsive in the case of F68, and exhibited a clear adhesion minimum for the more hydrophobic F127.

- Above the CAC, the onset of the interaction forces increases dramatically with the experimental run/immersion time. The binding of the polymers to the bilayers is now very strong, especially for F127, which possesses a larger hydrophobic segment compared to F68. The force runs exhibit a pronounced plateau around $F/R \approx 10$ mN/m ($E \approx 1.6$ mJ/m^2), indicating the collapse or disruption of the cohesive polymer layers on the bilayers upon compression. The decay length of the long-range interaction force profiles now scales with the hydrodynamic radius of the polymer aggregate. Adhesive forces
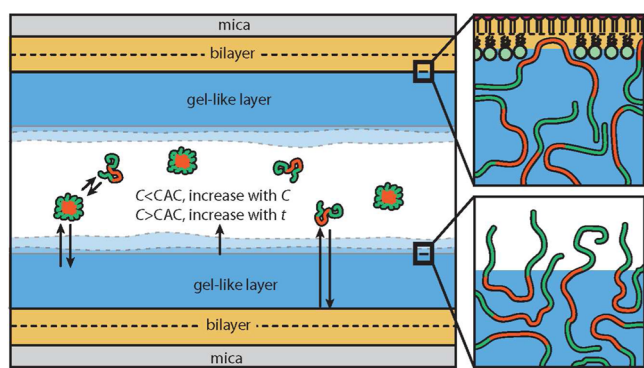
Figure 6. Schematic representation of the different processes observed in the presence of Pluronic polymers. At $C < $ CAC, the gel-like layer is very thin and poorly anchored to the lipid bilayer except for the more hydrophobic polymer, F127. At $C > $ CAC, the thickness of the gel layer increases with time due to addition of polymer aggregates from the bulk.

between the adsorbed polymer layers increase with immersion time (see Figure 6).

From our experiments it is clear that bridging attraction between bilayers is hard to rule out in certain cases. In the presence of PEG, the position of the contact position (hard wall thickness) after the attractive jump is identical to the hard wall thickness without any polymer in solution, suggesting that all the polymer has been removed from the surfaces, ruling out any bridging attraction. In the presence of pluronics, certain clues suggest that bridging is not the primary mechanism in the observed adhesion. Bridging would manifests itself by an onset of (attractive) interaction close to the size of the extended

molecules (10 nm or more), which was never observed (ΔD_{jump} were always smaller than 10 nm). In the case of bridging by physisorbed segments, the interaction force is expected to be linear and attractive over a range close to the contour length of the polymer chain, which was not observed either.

Most of these observations echo recently published reports using similar systems. For example, experimental and simulation studies have shown that pluronic polymers can interact with lipid bilayers via their hydrophobic domains, which are able to penetrate into bilayers and to fluidize them.[34,35,38,39] Even though these studies are usually performed on unsupported bilayers (mainly free lipid vesicles in solution), which allow translocation of the polymer through the bilayer in contrast to supported bilayers, the results are in qualitative agreement with our observations, especially at $C < $ CAC.

Studies performed at high polymer concentrations are more scarce and therefore difficult to compare with. Recently, Hugouvieux and Kolb[40] reported a simulation study detailing the structure of adsorbed films of multiblock copolymers at the bilayer/fluid interface over a wide range of polymer concentrations. The authors showed that micellar aggregates can adhere at the surface of lipid bilayers. These aggregates tend to organize on the bilayer as the concentration of polymer is increased until these percolate into a continuous gel-like layer sitting on top of the bilayer and anchor to it via polymer bridges of isolated chains. Interestingly, the authors showed that two time scales tend to govern this process: a short characteristic time corresponding to the formation of the micellar aggregates in the bulk and at the surface, and a long characteristic time corresponding to the exchange of polymer chains between the bulk and the bilayers. These results are in remarkable agreement with our observations, especially at $C \gg $ CAC, where we systematically observed the presence of a gel-like layer strongly anchored on the bilayers. Our SFA data also confirmed that the gel layer can be highly structured, as shown by the FECO fringe analysis under high compression, and that the layer formation is a dynamic process that extends over a few hours.

The interpretation of our results did not consider at any point the lipid composition of the bilayers. In the case of the experiments with PEG, the agreement between our results and a previous report by Kuhl et al.[32,33] performed on a totally different bilayer system strongly suggests that the depletion interaction does not depend significantly on the lipid composition. Experiments performed with Pluronics might indeed depend on the lipid composition, especially when $C < $ CAC. In this concentration regime, the lipid bilayer was observed to be thin and polymers to be inserted into the bilayers. Both processes are expected to depend on the lipid composition and bilayer structure/domains. We can easily speculate that the polymer hydrophobic segments will not have the same penetration capacity, and therefore anchoring strength, in a condensed lipid phase compared to the liquid expanded phase.

On a larger perspective, the present study suggest that Pluronic polymers might not be the candidates of choice to promote adhesion between biological membranes. Our results show that Pluronics tend to accumulate at the surface of the membrane, forming a structured gel coating that does not promote any significant adhesion between the membranes but rather repulsion. This behavior is characteristic of a membrane-protecting agent or a membrane sealant. Such observation seems to be in line with numerous studies reporting the protecting role of Pluronics against membrane damage, as seen in

induced brain injury,[41,42] brain ischemia,[43] or ischemic spinal cord injury.[44] PEG on the other hand appears to be an interesting candidate, considering that the adhesive strength between the membranes can be modulated directly by the polymer concentration. As we showed, PEG-mediated membrane adhesion uses depletion forces that rely on the expulsion of the polymer from the contact zone. Such mechanism can be advantageous compared to other polymer mediated adhesive mechanisms such as polymer bridging, which are limited by the saturation concentration of the polymer at the surface. Even though PEG-induced depletion forces represent an attractive option to promote membranes adhesion, its use in biomedical settings might be limited due to the extremely high concentrations necessary to achieve significant adhesion. Even for a well-tolerated polymer such as PEG, high concentrations might induce severe inflammatory and immune responses. Biodegradable and biocompatible polymers should be an attractive alternative to avoid this problem.

■ CONCLUSION

In conclusion, our experimental results shed new light on the interaction forces between lipid bilayers in the presence of PEG-based polymers and illustrate the subtle behavior of these particular polymers at the lipid/fluid interface. We anticipate that our observations and their molecular scale interpretation will guide the development of future applications of such polymers, especially in the biopharmaceutical and biomedical fields.

■ ASSOCIATED CONTENT

Ⓢ Supporting Information

The Supporting Information is available free of charge on the ACS Publications website at DOI: 10.1021/acs.biomac.5b01216.

Bilayer−bilayer interaction profiles (PDF)

■ AUTHOR INFORMATION

Corresponding Authors

*E-mail: xavier.banquy@umontreal.ca; Phone: (514) 343-2470; Fax: (514) 343-2102.
*E-mail: Jacob@engineering.ucsb.edu; Phone: (805) 893-8407; Fax: (805) 893-7870.

Notes

The authors declare no competing financial interest.

■ ACKNOWLEDGMENTS

■ REFERENCES

(1) Allen, C.; Maysinger, D.; Eisenberg, A. *Colloids Surf., B* **1999**, *16*, 3−27.
(2) Batrakova, E. V.; Kabanov, A. V. *J. Controlled Release* **2008**, *130*, 98−106.
(3) Johnsson, M.; Silvander, M.; Karlsson, G.; Edwards, K. *Langmuir* **1999**, *15*, 6314−6325.
(4) Mina, E. W.; Lasagna-Reeves, C.; Glabe, C. G.; Kayed, R. *J. Mol. Biol.* **2009**, *391*, 577−585.
(5) Spurney, C. F.; Guerron, A. D.; Yu, Q.; Sali, A.; van der Meulen, J. H.; Hoffman, E. P.; Nagaraju, K. *BMC Cardiovasc. Disord.* **2011**, *11*, 20.
(6) Batrakova, E. V.; Li, S.; Alakhov, V. Y.; Miller, D. W.; Kabanov, A. V. *J. Pharmacol. Exp. Ther.* **2003**, *304*, 845−854.

(7) Batrakova, E. V.; Li, S.; Vinogradov, S. V.; Alakhov, V. Y.; Miller, D. W.; Kabanov, A. V. *J. Pharmacol. Exp. Ther.* **2001**, *299*, 483−493.
(8) Parnaud, G.; Taché, S.; Peiffer, G.; Corpet, D. E. *Br. J. Cancer* **2001**, *84*, 90.
(9) Khattak, S. F.; Bhatia, S. R.; Roberts, S. C. *Tissue Eng.* **2005**, *11*, 974−983.
(10) Batrakova, E. V.; Han, H.-Y.; Miller, D. W.; Kabanov, A. V. *Pharm. Res.* **1998**, *15*, 1525−1532.
(11) Marra, J.; Israelachvili, J. *Biochemistry* **1985**, *24*, 4608−4618.
(12) Israelachvili, J. N. *Intermolecular & Surface Forces*; Elsevier Academic Press: San Diego, CA, 2011.
(13) Borgens, R. B.; Bohnert, D.; Duerstock, B.; Spomar, D.; Lee, R. C. *J. Neurosci. Res.* **2004**, *76*, 141−154.
(14) Borgens, R. B.; Bohnert, D. *J. Neurosci. Res.* **2001**, *66*, 1179−1186.
(15) Laverty, P. H.; Leskovar, A.; Breur, G. J.; Coates, J. R.; Bergman, R. L.; Widmer, W. R.; Toombs, J. P.; Shapiro, S.; Borgens, R. B. *J. Neurotrauma* **2004**, *21*, 1767−1777.
(16) Ohler, B.; Graf, K.; Bragg, R.; Lemons, T.; Coe, R.; Genain, C.; Israelachvili, J.; Husted, C. *Biochim. Biophys. Acta, Mol. Basis Dis.* **2004**, *1688*, 10−17.
(17) Linegar, K. L.; Adeniran, A. E.; Kostko, A. F.; Anisimov, M. A. *Colloid J.* **2010**, *72*, 279−281.
(18) Alexandridis, P.; Lindman, B. *Amphiphilic Block Copolymers: Self-Assembly and Applications*; Elsevier: Amsterdam, 2000.
(19) Endo, H.; Yamamoto, M. *Polym. J.* **1974**, *6*, 356−363.
(20) Kabanov, A. V.; Batrakova, E. V.; Miller, D. W. *Adv. Drug Delivery Rev.* **2003**, *55*, 151−64.
(21) Israelachvili, J. N.; Min, Y.; Akbulut, M.; Alig, A. G.; Carver, G.; Greene, W.; Kristiansen, K.; Meyer, E. E.; Pesika, N. S.; Rosenberg, K.; Zeng, H. *Rep. Prog. Phys.* **2010**, *73*, 036601−17.
(22) Min, Y.; Kristiansen, K.; Boggs, J. M.; Husted, C.; Zasadzinski, J. A.; Israelachvili, J. N. *Proc. Natl. Acad. Sci. U. S. A.* **2009**, *106*, 3154−3159.
(23) Banquy, X.; Kristiansen, K.; Lee, D. W.; Israelachvili, J. N. *Biochim. Biophys. Acta, Biomembr.* **2012**, *1818*, 402−410.
(24) Lee, D. W.; Banquy, X.; Kristiansen, K.; Kaufman, Y.; Boggs, J. M.; Israelachvili, J. N. *Proc. Natl. Acad. Sci. U. S. A.* **2014**, *111*, E768−E775.
(25) Leckband, D. E.; Helm, C. A.; Israelachvili, J. *Biochemistry* **1993**, *32*, 1127−1140.
(26) Israelachvili, J. N. *J. Colloid Interface Sci.* **1973**, *44*, 259−272.
(27) Israelachvili, J. N.; Adams, G. E. *J. Chem. Soc., Faraday Trans. 1* **1978**, *74*, 975.
(28) Horn, R. G.; Israelachvili, J. N.; Pribac, F. *J. Colloid Interface Sci.* **1987**, *115*, 480−492.
(29) Banquy, X.; Lee, D. W.; Das, S.; Hogan, J.; Israelachvili, J. N. *Adv. Funct. Mater.* **2014**, *24*, 3152−3161.
(30) Bureau, L. *Phys. Rev. Lett.* **2007**, *99*, 225503.
(31) Ruths, M.; Israelachvili, J. N.; Ploehn, H. J. *Macromolecules* **1997**, *30*, 3329−3339.
(32) Kuhl, T. L.; Berman, A. D.; Hui, S. W.; Israelachvili, J. N. *Macromolecules* **1998**, *31*, 8250−8257.
(33) Kuhl, T.; Guo, Y.; Alderfer, J. L.; Berman, A. D.; Leckband, D.; Israelachvili, J.; Hui, S. W. *Langmuir* **1996**, *12*, 3003−3014.
(34) Hezaveh, S.; Samanta, S.; De Nicola, A.; Milano, G.; Roccatano, D. *J. Phys. Chem. B* **2012**, *116*, 14333−14345.
(35) Demina, T.; Grozdova, I.; Krylova, O.; Zhirnov, A.; Istratov, V.; Frey, H.; Kautz, H.; Melik-Nubarov, N. *Biochemistry* **2005**, *44*, 4042−4054.
(36) Cheng, C. Y.; Wang, J. Y.; Kausik, R.; Lee, K. Y. C.; Han, S. *Biomacromolecules* **2012**, *13*, 2624−2633.
(37) Cheng, C. Y.; Wang, J. Y.; Kausik, R.; Lee, K. Y. C.; Han, S. *J. Magn. Reson.* **2012**, *215*, 115−119.
(38) Nawaz, S.; Redhead, M.; Mantovani, G.; Alexander, C.; Bosquillon, C.; Carbone, P. *Soft Matter* **2012**, *8*, 6744−6754.
(39) Wang, J. Y.; Chin, J. M.; Marks, J. D.; Lee, K. Y. C. *Langmuir* **2010**, *26*, 12953−12961.
(40) Hugouvieux, V.; Kolb, M. *Langmuir* **2014**, *30*, 12400−12410.
(41) Cadichon, S. B.; Le, H. M.; Wright, D. A.; Curry, D. J.; Kang, U.; Frim, D. M. *J. Neurosurg* **2007**, *106*, 36−40.

(42) Curry, D. J.; Wright, D. A.; Lee, R. C.; Kang, U. J.; Frim, D. M. *J. Neurosurg* **2004**, *101*, 91−6.

(43) Shelat, P. B.; Plant, L. D.; Wang, J. C.; Lee, E.; Marks, J. D. *J. Neurosci.* **2013**, *33*, 12287−99.

(44) Follis, F.; Jenson, B.; Blisard, K.; Hall, E.; Wong, R.; Kessler, R.; Temes, T.; Wernly, J. *Journal of investigative surgery: the official journal of the Academy of Surgical Research* **1996**, *9*, 149−56.